

# Inverse scattering internal multiple attenuation algorithm in complex multi-D media: the pseudo-depth/vertical-time monotonicity condition and higher dimension analytic analysis

Bogdan G. Nita and Arthur B. Weglein

## Abstract

In this paper we discuss the multi-D inverse scattering internal multiple attenuation algorithm focusing our attention on the prediction mechanisms. Roughly speaking, the algorithm combines amplitude and phase information of three different arrivals (sub-events) in the data set to predict one interbed multiple. The three events are conditioned by a certain relation which requires that their pseudo-depths, defined as the depths of their turning points relative to the constant background velocity, satisfy a lower-higher-lower relationship. This implicitly assumes a pseudo-depth monotonicity condition, i.e. the relation between the actual depths and the pseudo-depths of any two sub-events, is the same. We study the lower-higher-lower relation in pseudo-depth and show that it is directly connected with a similar longer-shorter-longer relationship between the vertical or intercept times of the sub-events and hence the pseudo-depth monotonicity is equivalent to a vertical time monotonicity condition. The paper also provides the first pre-stack analysis of the algorithm with analytical data showing how the sub-events are selected and combined to exactly predict the time and well approximate the amplitude of an interbed multiple. Among other results we show that the construction of internal multiples is performed in the plane waves domain and, as a consequence, the internal multiples with head-waves sub-events are also predicted by the algorithm. Furthermore we analyze the differences between the time monotonicity condition in vertical or intercept time and total travel time and show a 2D example which satisfies the former (and hence is predicted by the algorithm) but not the latter. Finally we discuss one case in which the monotonicity condition is not satisfied by the sub-events of an internal multiple which, as a consequence, will not be predicted. For these cases, the monotonicity condition turns out to be too restrictive and we discuss ways of lowering these restrictions and hence expanding the algorithm to address these types of multiples.

## Introduction

The inverse scattering series is presently the only multidimensional method for inverting for the properties of an unknown medium without adequate information about that medium. When the series converges it achieves full inversion given the whole data set (including free surface and internal multiples) and information about a chosen reference medium. Carvalho (6) tested numerically the convergence properties of the full inverse scattering series and found that the series converges only when the reference medium of choice is within 11% from the actual medium, a non-realistic situation. In the '90's, Weglein and collaborators developed the "subseries method" (for a history and description see (20)) which consists in identifying task specific subseries in the full series, with targeted usefulness and better convergence properties than the whole series. These subseries were imagined to be a sequence of steps, similar to the processing steps undertaken in geophysical exploration, which would achieve 1. Free surface multiple elimination; 2. Internal multiple elimination;

3. Imaging in depth; and 4. Inversion for the medium properties. It is reasonable to assume, and the experience showed this assumption to be true, that since the full series only requires data and information about a reference medium to invert, the same holds for any of the four specific subseries.

The inverse scattering series, and the subsequent task specific subseries, assume that the input data satisfies several pre-requisites. First, it is assumed that the source signature or wavelet has been deconvolved from the data. Second, both the source and receiver ghosts have been eliminated from the collected data. Third, the collected data itself has an appropriate sampling or the data reconstruction algorithms are able to improve the acquisition sampling to an appropriate degree. When these prerequisites are not satisfied, the algorithms derived from this method will reach incorrect conclusions/results e.g. false or no prediction of free-surface and internal multiples, incorrect location of subsurface structures, and errors in parameter estimation. Last but not least we mention that the algorithms are derived from a point-source point-receiver wave theory approach and any deviations from that, e.g. source and receiver arrays, would have to be studied to understand how they affect the algorithms.

In 1994, Araujo (2) identified the first term in the subseries for internal multiple elimination (see also (19)). This first term by itself exactly predicts the time of arrival, or phase, and well approximates the amplitude of internal multiples, without being larger than the actual amplitude, and hence it represents an algorithm for *attenuation*. Weglein et al. (20) described the algorithm through an analytic 1D example and 2D synthetic numerics. Field data tests were also performed showing an extraordinary ability to predict difficult interbed multiples, e.g. superimposed primary and multiple etc., where other methods have failed.

The inverse scattering internal multiple attenuation algorithm was found through a combination of simple 1D models testing/evaluation and certain similarities between the way the data is constructed by the forward scattering series and the way arrivals in the data are processed by the inverse scattering series. This connection between the forward and the inverse series was analyzed and described by Matson (10), (11) and Weglein et al. (19), (20). Specifically, they showed that an internal multiple in the forward scattering series is constructed by summing certain types of scattering interactions which appear starting with the third order in the series. The piece of this term representing the first order approximation to an internal multiple is exactly the one for which the point scatterers satisfy a certain lower-higher-lower relationship in actual depth. Summing over all interactions of this type in the actual medium results in constructing the first order approximation to an internal multiple. By analogy, it was inferred that the first term in the subseries for eliminating the internal multiples would be one constructed from events satisfying the same lower-higher-lower relationship in pseudo-depth. The assumption that the ordering of the actual and the pseudo depths of two sub-events is preserved, i.e.

$$z_1^{actual} < z_2^{actual} \iff z_1^{pseudo} < z_2^{pseudo}, \quad (1)$$

has been subsequently called “the pseudo-depth monotonicity condition”.

In this paper we further analyze this relation and show that it is equivalent to a vertical or intercept time (here denoted by  $\tau$ ) monotonicity condition

$$z_1^{actual} < z_2^{actual} \iff \tau_1 < \tau_2, \quad (2)$$

for any two sub-events. We also look at the differences between the time monotonicity condition in vertical or intercept time and total travel time. The latter was pointed out by a different algorithm derived from the inverse scattering series by ten Kroode (17) and further described by Malcolm and M.V. de Hoop (9). We show a 2D example which satisfies the former (and hence is predicted by the original algorithm) but not the latter. Finally we discuss one case in which the monotonicity condition is not satisfied by the sub-events of an internal multiple in either vertical or total travel time and consequently the multiple will not be predicted by either one of the two algorithms. For these cases, the monotonicity condition turns out to be too restrictive and we discuss ways of lowering these restrictions and hence expanding the algorithm to address these types of multiples.

In the context of the overall research efforts of M-OSRP, this paper represents a part of a project to characterize, implement, and build on the internal multiple attenuation algorithm that is reported on in this volume. Kaplan et al. (8) describe the development of a practical code to effect numerical examples of this de-multiple procedure in 1D prestack and 2D regimes; they further detail mathematically- and physically-based representations of the algorithm that lead to reduced computation time. Ramírez and Weglein (13) meanwhile work to progress towards a method for the elimination of interbed multiples through an analysis and incorporation of specific higher-order terms that yet mimic the pseudo-depth relationships we discuss herein. Ramírez and Weglein (14) concern themselves with the characterization of the attenuative nature of the algorithm. Here we provide a characterization of a different sort, as summarized above.

The paper is structured as follows. In Section 2 we will discuss the definition of a multiple and its evolution over time. In Section 3 we will describe the algorithm and show how a predicted multiple is constructed from events in the data. A 1.5D example is analyzed in Section 4 with analytical data and internal multiples with headwaves sub-events are shown to be predicted by the algorithm. We further look in Sections 5 and 6 at several 2D examples to better understand the relationship between the sub-events which are used by the algorithm to construct the phase and the amplitude of the internal multiple. Some comments and conclusions are presented in the last section.

## Definition of an internal multiple

The definition of an internal multiple evolved over time keeping in step with our understanding of fundamental structure and processes that take place inside a medium. Once a certain definition is in place, one can then start the development of algorithms which address the so called (and defined) internal multiples to attenuate or even eliminate them. However, sometimes, after an algorithm is developed, its analysis leads to new definitions or generalizations of the notions/concepts themselves. This was the case of the inverse scattering internal multiple algorithm and the definitions resulted from it will be discussed in this section.

The early 1D models of a layered medium only allow up and down propagation and so it is easy to imagine a primary as having only one upward reflection and a multiple as having two or more upward reflection and one or more internal (i.e. not at the free surface) downward reflections. Notice that the directions up and down are defined by the positioning of the measurement surface: if an event is propagating towards the measurement surface it is said that it is moving upward. If the event is moving away from the measurement surface it is said that it is moving downward. In our discussion/pictures, we choose the  $x$ -axis to be along the measurement surface and hence the up-down direction to coincide with moving backward and forward along the  $z$ -axis.

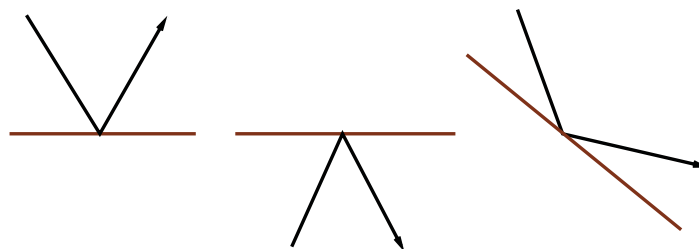


Figure 1: An example of an upward, downward and a neutral reflection.

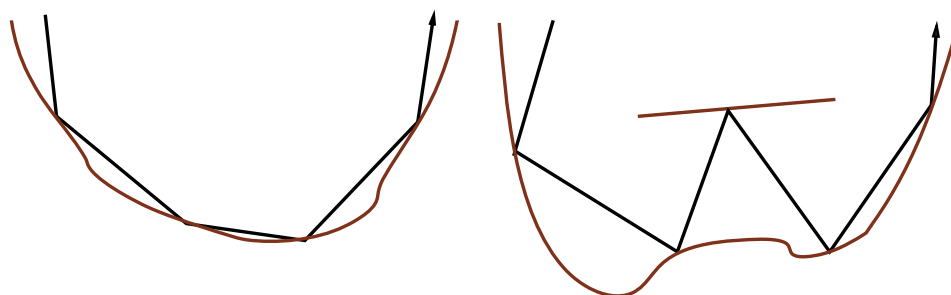


Figure 2: A more general definition of a primary and a multiple. The primary has one upward reflection and any number of neutral reflections while the multiple has two or more upward reflections and any number of neutral reflections.

When the medium is slightly more general, for example a 2D medium with only specular reflections, a new type of reflection occurs which is neither upward nor downward (see Figure 1). We will call this type of reflection a neutral reflection. For this situation we can easily generalize the definition of a primary as an event which contains one upward reflection and any number of neutral reflections and that of a multiple as an event which has two or more upward reflections, one or more downward reflections and any number of neutral reflections (an example is shown in Figure 2). However this definition does not cover the complexity of an arbitrary medium and there are events which do not fit the definition of a multiple as given so far. For example, the events pictured in Figure 3 (a)(b) do not have two upward reflections but a turning wave and a headwave respectively, while the event in Figure 3(c) is even of a more complex nature consisting in a diffraction on one leg of the full event. Recently, Weglein and Dragoset (21) have introduced more general definitions and designations for primary and multiply reflected events, namely prime and composite events. According to those definitions, a *prime event* is not decomposable into other recorded events such that those sub-event ingredients combine by adding and/or subtracting time of arrival to produce the prime. A *composite event* is composed of sub-events that combine in the above described manner to produce the event. With these definitions, the events pictured in Figure 3 can be categorized as composite events when their sub-events can be found in the recorded data. For example, the sub-events of the event pictured in Figure 3(a) are the turning wave and the reflections from the shallow and deep interfaces.

These definitions, which obviously generalize all the previous ones, and the notion of sub-events were suggested by the inverse scattering internal multiple attenuation algorithm which is going to be discussed in detail in the next sections.

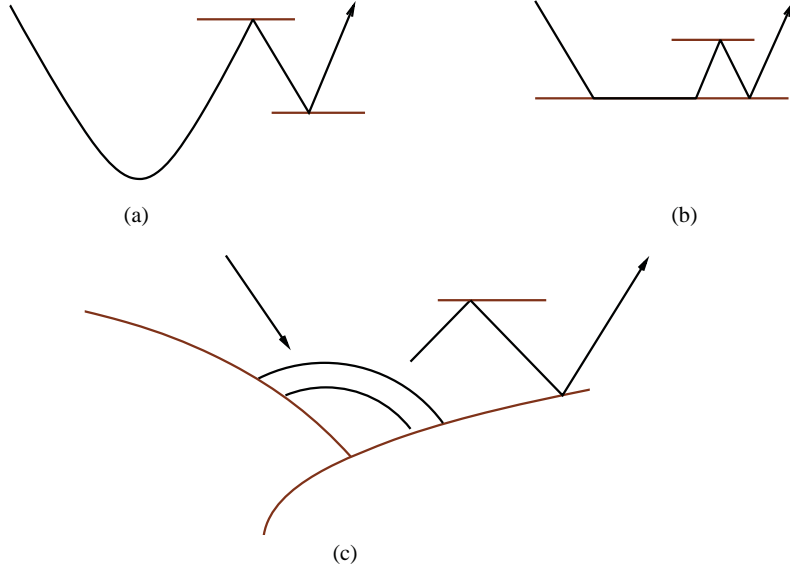


Figure 3: *Complex events difficult to include in a definition which only takes into account upward and downward reflections*

## The inverse scattering series internal multiple attenuation algorithm

The first term in the inverse scattering subseries for internal multiple elimination is (see e.g. (20))

$$\begin{aligned}
 b_3(k_g, k_s, \omega) &= \frac{1}{(2\pi)^2} \int_{-\infty}^{\infty} \int_{-\infty}^{\infty} dk_1 e^{-iq_1(\epsilon_g - \epsilon_s)} dk_2 e^{iq_2(\epsilon_g - \epsilon_s)} \int_{-\infty}^{\infty} dz_1 e^{i(q_g + q_1)z_1} b_1(k_g, k_1, z_1) \\
 &\times \int_{-\infty}^{z_1} dz_2 e^{i(-q_1 - q_2)z_2} b_1(k_1, k_2, z_2) \int_{z_2}^{\infty} dz_3 e^{i(q_2 + q_s)z_3} b_1(k_2, k_s, z_3)
 \end{aligned} \quad (3)$$

where  $z_1 > z_2$  and  $z_2 < z_3$  and  $b_1$  is defined in terms of the original pre-stack data with free surface multiples eliminated,  $D'$ , to be

$$D'(k_g, k_s, \omega) = (-2iq_s)^{-1} B(\omega) b_1(k_g, k_s, q_g + q_s) \quad (4)$$

with  $B(\omega)$  being the source signature. Here  $k_s$  and  $k_g$  are horizontal wavenumbers, for source and receiver coordinates  $x_s$  and  $x_g$ , and  $q_g$  and  $q_s$  are the vertical wavenumbers associated with them. The  $b_3$  on the left hand side represents the first order prediction of the internal multiples. An internal multiple in  $b_3$  is constructed through the following procedure.

The deconvolved data without free-surface multiples in the space-time domain,  $D(x_s, x_g, t)$  can be described as a sum of Dirac delta functions

$$D(x_s, x_g, t) = \sum_a R_a \delta(t - t_a) \quad (5)$$

representing different arrivals (primaries and internal multiples). Here  $R_a$  represents the amplitude of each arrival and it is a function of source and receiver position  $x_s$  and  $x_g$  and frequency  $\omega$ . When transformed to the frequency domain the transformed function  $D(x_s, x_g, \omega)$  is a sum

$$\tilde{D}(x_s, x_g, \omega) = \sum_a \tilde{R}_a e^{-i\omega t_a}. \quad (6)$$

Here  $t_a$  is the total traveltime for each arrival and it can be thought of as a sum of horizontal and vertical times  $t_a = \tau_a + t_{xa}$  (see e.g. (7), (18)), where  $t_{xa}$  is a function of  $x_g$  and  $x_s$ . After Fourier transforming over  $x_s$  and  $x_g$ , the data is  $\tilde{D}(k_s, k_g, \omega)$ . The transforms act on the amplitude as well as on the phase of the data and transform the part of the phase which is described by the horizontal time  $t_{xa}$ . Hence  $D(k_s, k_g, \omega)$  can now be thought of as a sum of terms containing  $e^{i\omega\tau_a}$  with  $\tau_a$  being the vertical or intercept time of each arrival

$$\tilde{D}(k_s, k_g, \omega) = \sum_a \tilde{R}'_a e^{-i\omega\tau_a} \quad (7)$$

and where  $\tilde{R}'_a$  is the double Fourier transform over  $x_g$  and  $x_s$  of  $\tilde{R}_a e^{-i\omega t_{xa}}$ . The multiplication by the obliquity factor,  $2iq_s$ , changes the amplitude of the plane wave components without affecting the phase; hence  $b_1(k_s, k_g, \omega)$  represents an effective plane wave decomposed data and is given by

$$b_1(k_s, k_g, \omega) = \sum_a \tilde{R}''_a e^{-i\omega\tau_a} \quad (8)$$

where  $\tilde{R}''_a = 2iq_s \tilde{R}'_a$  and whose phase,  $e^{i\omega\tau_a}$ , contains information only about the recorded *actual* vertical or intercept time.

Notice that for each planewave component of fixed  $k_s$ ,  $k_g$  and  $\omega$  we have

$$\omega\tau_a = k_z^{actual} z_a^{actual} \quad (9)$$

where  $k_z^{actual}$  is the actual, velocity dependent, vertical wavenumber and  $z_a^{actual}$  is the actual depth of the turning point of the planewave. Since the velocity of the actual medium is assumed to be unknown, this relationship is written in terms of the reference velocity as

$$\omega\tau_a = k_z z_a \quad (10)$$

where  $k_z$  is the vertical wavenumber of the planewave in the reference medium,  $k_z = \sqrt{\frac{\omega}{c_0} - k_s} + \sqrt{\frac{\omega}{c_0} - k_g}$ , and  $z_a$  is the pseudo-depth of the turning point. This implicit operation in the algorithm is performed by denoting  $b_1(k_s, k_g, \omega) = b_1(k_s, k_g, k_z)$  with the latter having the expression

$$b_1(k_s, k_g, k_z) = \sum_a \tilde{R}''_a e^{-ik_z z_a}. \quad (11)$$

The next step is to Inverse Fourier Transform over the reference  $k_z$  hence obtaining

$$b_1(k_s, k_g, z) = \int_{-\infty}^{\infty} e^{ik_z z} b_1(k_s, k_g, k_z) dk_z. \quad (12)$$

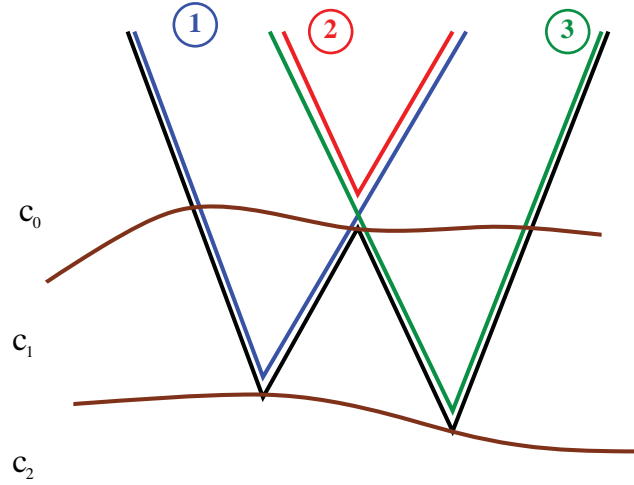


Figure 4: The sub-events of an internal multiple: the green, blue and red are arrivals in the data which satisfy the lower-higher-lower relationship in pseudo-depths  $z$ . The algorithm will construct the phase of the internal multiple shown in black by adding the phases of the green and the blue primaries and subtract the one of the red primary.

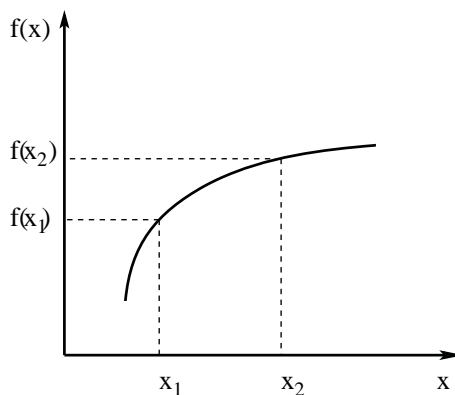
Putting together equations (11) and (12)) we find

$$b_1(k_s, k_g, z) = \sum_a \int_{-\infty}^{\infty} \tilde{R}''_a e^{ik_z(z-z_a)} dk_z \quad (13)$$

which represents a sum of delta-like events placed at pseudo-depths  $z_a$  and hence the  $b_1$  from the last equation is actually  $b_1(k_s, k_g, z_a)$ . This last step can also be interpreted as a downward continuation on both source and receiver sides, with the reference velocity  $c_0$ , and an imaging with  $\tau = 0$ , or, in other words, an un-collapsed F-K migration (see e.g. (15) and (16)). A discussion of differences in imaging with  $\tau$  and with  $t$  was given by Nita and Weglein (12).

Each internal multiple is constructed by considering three effective data sets  $b_1$  and searching, in the horizontal-wavenumber-pseudo-depth domain, for three arrivals which satisfy the lower-higher-lower relationship in their pseudo-depths, i.e.  $z_1 > z_2 < z_3$ , (see Figure 4 for an example of three such primary events). Having found such three arrivals in the data, the algorithm combines their amplitudes and phases to construct a multiple by adding the phases of the two pseudo-deeper events and subtracting the one of the pseudo-shallower ones and by multiplying their amplitudes. One can then see (see e.g. (20)) that the time of arrival of an internal multiple is exactly predicted and its amplitude is well approximated by this procedure.

As pointed out in the first section, the lower-higher-lower restriction was inferred from the analogy with the forward scattering series description of internal multiples: the first order approximation to an internal multiple (which occurs in the third term of the series) is built up by summing over all scattering interactions which satisfy a lower-higher-lower relationship in actual depth. The assumption that this relationship is preserved in going from actual depth to pseudo-depth is called “the pseudo-depth monotonicity condition”. (Recall that a monotonic function  $f(x)$  satisfies  $f(x_1) < f(x_2) \iff x_1 < x_2$ , see also Figure 5; here, we regard the pseudo-depth as a function of actual depth). Notice that the lower-higher-lower relationship in pseudo-depth can be translated,

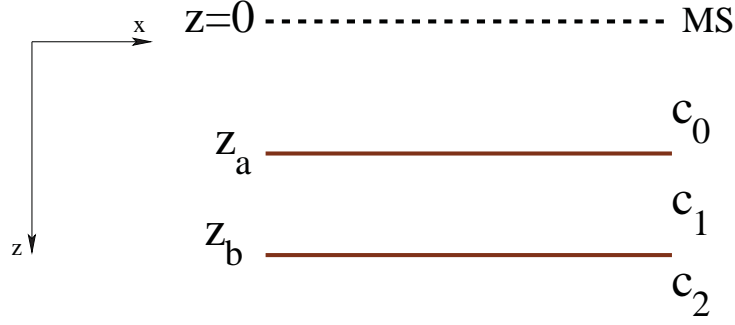
Figure 5: *A monotonic function.*

from equation (10), in a similar longer-shorter-longer relationship in the vertical or intercept time of the three events. Accordingly, the pseudo-depth monotonicity is also translated in a vertical time monotonicity condition. Notice that this is different from the total time monotonicity assumed by the algorithm introduced by ten Kroode (17). The latter is employing asymptotic evaluations of certain Fourier integrals which result in an algorithm in the space domain, having a ray theory assumption and the less inclusive total time monotonicity requirement. The justification for this approach was the attempt to attenuate a first order approximation to an internal multiple built by the forward scattering series. In contrast, the original algorithm is aimed at predicting and attenuating the actual multiples in the data and hence it takes into consideration the full wavefield, with no asymptotic compromises, and results in a more inclusive vertical time monotonicity condition. In Section 5 we discuss a 2D example in which the geometry of the subsurface leads to the existence of a multiple which satisfies the pseudo-depth/vertical-time but not the total time monotonicity condition.

In the next section we analyze a simple 1.5D example and show analytically how it predicts internal multiples by putting together amplitude and phase information from arrivals in the data satisfying the above condition. During this analysis we also show that the internal multiples with headwaves sub-events are attenuated by the algorithm.

## Attenuation of internal multiples with headwaves sub-events: a 1.5D example

The model in this experiment is a 2D vertically varying medium. We consider one of the simplest cases which allow the existence of internal multiples, namely one layer between two semi-infinite half-spaces separated by horizontal interfaces (see Figure 6). The velocity only varies across the interfaces located at  $z = z_a$  and  $z = z_b$  and has the values  $c_0$ ,  $c_1$  and  $c_2$  respectively. The sources and receivers are located at the same depth  $z = 0$ . The data for such a model is given in the

Figure 6: *The model for the 1.5D example.*

frequency  $\omega$  domain by (see e.g. (1))

$$D(x_h, 0; \omega) = \frac{1}{2\pi} \int_{-\infty}^{\infty} dk_h \frac{R_{01} + T_{01}R_{12}T_{10}e^{i\nu_1(z_b-z_a)} + \dots}{iq_s} e^{ik_h x_h} e^{ik_z z_a} \quad (14)$$

where  $k_z = q_g + q_s$ ,  $k_h = k_g + k_s$ ,  $x_h = \frac{x_g - x_s}{2}$  and  $\nu_1 = q_{1g} + q_{1s}$ . The reflection and transmission coefficients at the corresponding interfaces  $R_{01}$ ,  $T_{01}$ ,  $R_{12}$  and  $T_{10}$  are all functions of  $k_h$  and  $\omega$ . Only the primaries from the top and the bottom interfaces are written out explicitly in this equation; the dots “...” stand for other multiple arrivals. For simplicity we will drop the writing of the dots for the rest of this example; this will effect in the prediction of the first order internal multiple only.

Notice that the expression (14) represents both pre-critical and post-critical arrivals, as well as, for large offsets, headwaves along both interfaces. For a discussion of how to obtain the headwaves solutions from integrating Equation (14) see e.g. Aki and Richards (1) Chapter 6. The first order internal multiple that we seek to predict has the expression

$$IM_{actual}^{1st}(x_h, 0; \omega) = \frac{1}{2\pi} \int_{-\infty}^{\infty} dk_h \frac{T_{01}R_{12}^2 T_{10}R_{10}e^{2i\nu_1(z_b-z_a)}}{iq_s} e^{ik_h x_h} e^{ik_z z_a}. \quad (15)$$

This analytic formula contains both small and large offsets first order internal multiples arrivals including the multiples containing headwaves along the second interface as sub-events.

Fourier transforming the data given by equation (14) over  $x_h$  and  $x_m$  we find

$$D(k_h, 0; \omega) = \frac{R_{01} + T_{01}R_{12}T_{10}e^{-i\nu_1(z_b-z_a)}}{iq_s} e^{-ik_z z_a} \delta(k_g - k_s). \quad (16)$$

Then  $b_1(k_h, 0; \omega) = iq_s D(k_h, 0; \omega)$  is

$$b_1(k_h, 0; \omega) = \left[ R_{01} + T_{01}R_{12}T_{10}e^{-i\nu_1(z_b-z_a)} \right] e^{-ik_z z_a} \delta(k_g - k_s). \quad (17)$$

or

$$b_1(k_h, 0; \omega) = \left[ R_{01}e^{-ik_z z_a} + R'_{12}e^{-i\nu_1(z_b-z_a)}e^{-ik_z z_a} \right] \delta(k_g - k_s) \quad (18)$$

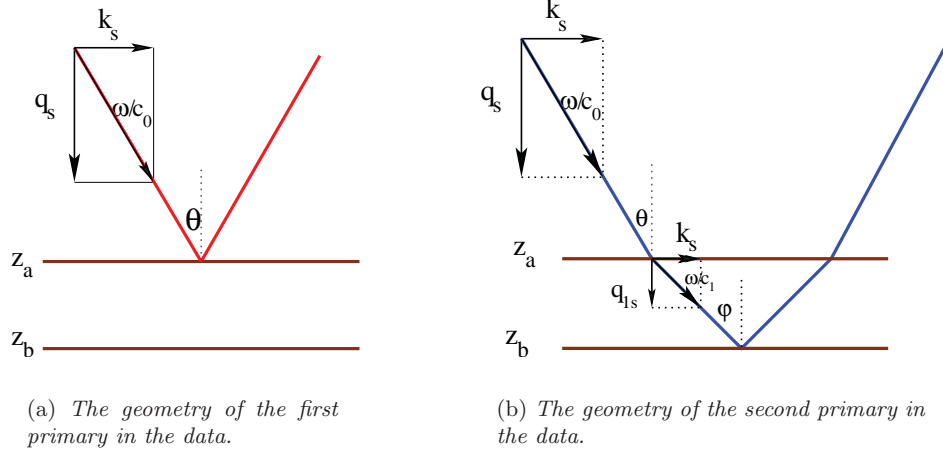


Figure 7: Geometrical representation of the two primaries.

where, for simplicity, we denoted  $T_{01}R_{12}T_{10} = R'_{12}$ .

For the first primary we can write (see Figure 7(a))  $\cos \theta = \frac{q_s}{\omega/c_0}$  which implies

$$q_s = \frac{\omega}{c_0} \cos \theta \quad (19)$$

or, noticing that  $\frac{c_0}{\cos \theta} = c_v^1$ , the vertical speed in the first medium,

$$q_s z_a = \frac{\omega}{c_0} z_a \cos \theta = \omega \frac{\tau^1}{2} \quad (20)$$

where  $\tau^1$  represents the intercept or vertical time of the first event. Similarly, on the receiver side we have

$$q_g z_a = \omega \frac{\tau^1}{2}. \quad (21)$$

Summing the last two equations we find for the first primary arrival (compare with equation 10)

$$k_z z_a = \omega \tau^1 \quad (22)$$

where we emphasize again that on the left hand side of the equation is the reference  $k_z$  and the pseudo-depth, which in this case coincides with the actual depth of the reflector,  $z_a$  and on the right hand side we have the phase information contained in the recorded data. For the second event we can find, as before, that, for the portion propagating through the space in between the measurement surface and the depth  $z_a$ , we have

$$k_z z_a = \omega \tau_1, \quad (23)$$

where  $\tau_1$  is the vertical time through the first medium. For the part that is propagating through the second medium we can write  $\cos \varphi = \frac{q_{1s}}{\omega/c_1}$  which implies

$$q_{s1} = \frac{\omega}{c_1} \cos \varphi, \quad (24)$$

or, noticing that  $\frac{c_1}{\cos\varphi} = c_v^2$ , the vertical speed in the layer,

$$q_{1s}(z_b - z_a) = \frac{\omega}{c_1}(z_b - z_a)\cos\varphi = \omega\frac{\tau_2}{2} \quad (25)$$

where  $\tau_2$  is the vertical time through the layer for this event. Similarly, on the receiver side we have

$$q_{1g}(z_b - z_a) = \omega\frac{\tau_2}{2}. \quad (26)$$

Summing the last two equations we find

$$\nu_1(z_b - z_a) = \omega\tau_2. \quad (27)$$

Summarizing, for the second primary we found from equations (23) and (27)

$$k_z z_a + \nu_1(z_b - z_a) = \omega\tau^2 \quad (28)$$

where  $\tau^2$  is the total vertical time for the second event.

Since the velocity of the second medium is not known, we can write  $\omega\tau^2$  in terms of  $c_0$  only as follows (see Equation (10))

$$\omega\tau^2 = k_z z'_b \quad (29)$$

where  $z'_b$  is a pseudo-depth which can be calculated in terms of the vertical time  $\tau^2$  and the vertical speed of the first medium. With these remarks, the expression (18) for  $b_1$  becomes

$$b_1(k_h, 0; \omega) = \left[ R_{01}e^{-ik_z z_a} + R'_{12}e^{-ik_z z'_b} \right] \delta(k_g - k_s) \quad (30)$$

To calculate  $b_1(k_h, z)$  we first downward continue/extrapolate,

$$b_1(k_h, z; \omega) = \left[ R_{01}e^{ik_z(z-z_a)} + R'_{12}e^{ik_z(z-z'_b)} \right] \delta(k_g - k_s), \quad (31)$$

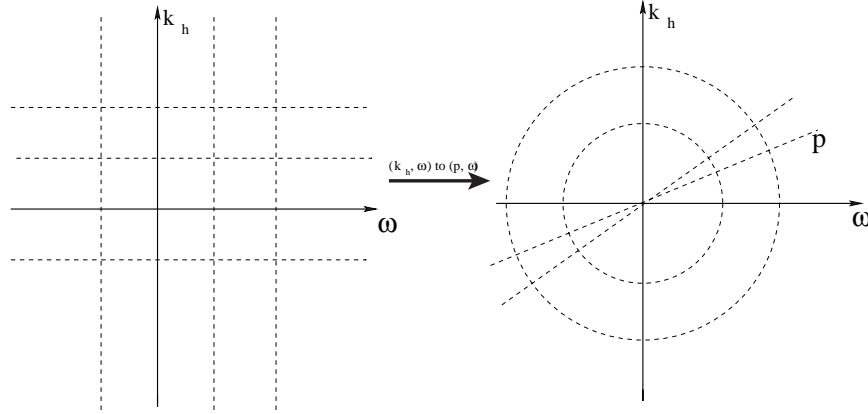
and then integrate over  $k_z$  (imaging) to obtain

$$b_1(k_h, z) = \int_{-\infty}^{\infty} dk_z b_1(k_h, k_z; \omega). \quad (32)$$

Notice that the reflection and transmission coefficients in the expression (31) are functions of  $\omega$  and hence functions of  $k_z$ . Explicitly,

$$R_{01}(k_h, \omega) = \frac{\sqrt{\frac{4\omega^2}{c_0^2} - k_h^2} - \sqrt{\frac{4\omega^2}{c_1^2} - k_h^2}}{\sqrt{\frac{4\omega^2}{c_0^2} - k_h^2} + \sqrt{\frac{4\omega^2}{c_1^2} - k_h^2}}. \quad (33)$$

The integration over  $k_z$  in (32) hence amounts to an inverse Fourier transform of  $R_{01}$  and  $R'_{12}$  over  $k_z$ . This Fourier transform is difficult to write as an analytic result and hence the example can no longer continue in the  $(k_h, \omega)$  domain.

Figure 8: The mapping  $(k_h, \omega)$  to  $(p, \omega)$ 

The imaging of the data can also be achieved in the  $(p, \omega)$  domain with better analytical results and more meaningful amplitude analysis (see Bruin et al (1990)). To this end we map the data from the  $(k_h, \omega)$  to  $(p, \omega)$  domain. This mapping has been studied extensively by Bracewell (1956) and Bracewell and Riddle (1967). It mainly consists in reading the data along the lines going through the origin of the  $(k_h, \omega)$  coordinate system instead of the original  $(k_h, \omega)$  grid (see Figure 8). Notice that, if this mapping is performed, the reflection and the transmission coefficients are no longer dependent of the frequency  $\omega$  or  $k_z$ . Explicitly, in the formula (33) for  $R_{01}$  we can factor  $\omega$  and then divide by it and so the expression becomes

$$R_{01}(p) = \frac{\sqrt{\frac{4}{c_0^2} - p^2} - \sqrt{\frac{4}{c_1^2} - p^2}}{\sqrt{\frac{4}{c_0^2} - p^2} + \sqrt{\frac{4}{c_1^2} - p^2}}. \quad (34)$$

Similarly it can be shown that  $R'_{12}$  is mapped to a function of  $p$  only.

In this new coordinate system the imaging step reads

$$b_1(p, z) = \int_{-\infty}^{\infty} dk_z b_1(p, k_z; \omega) = [R_{01}(p)\delta(z - z_a) + R'_{12}(p)\delta(z - z'_b)] \delta(k_g - k_s). \quad (35)$$

Numerical results comparing imaging in  $(k_h, \omega)$  and  $(p, \omega)$  were shown and discussed in Bruin et al. (1990). The imaged data written in equation (35) is next taken through the internal multiple algorithm described in equation (3).

Given the data in the form (35), the algorithm performs similarly to the 1D normal incidence case. In the following, we are denoting by  $p_1$ ,  $p_2$  and  $p_3$  the horizontal slownesses associated with  $k_g + k_1$ ,  $k_2 + k_s$  and  $k_g + k_s$  respectively. The horizontal slowness associated with  $k_s + k_g$  is also denoted by  $p$ . The four slownesses defined above are not independent, in fact we have that  $p_3 = (p_1 + p_2) - p$ .

The inner most integral towards calculating  $b_3$  in the internal multiple algorithm is

$$\begin{aligned}
& \int_{z'_2 + \varepsilon_1}^{\infty} dz'_3 e^{ik_z z'_3} [R_{01}(p_2)\delta(z'_3 - z_a) + R'_{12}(p_2)\delta(z'_3 - z'_b)] \delta(k_2 - k_s) \\
&= \int_{-\infty}^{\infty} dz'_3 H(z'_3 - (z'_2 + \varepsilon_1)) e^{ik_z z'_3} [R_{01}(p_2)\delta(z'_3 - z_a) + R'_{12}(p_2)\delta(z'_3 - z'_b)] \delta(k_2 - k_s) \\
&= \left[ H(z_a - (z'_2 + \varepsilon_1)) R_{01}(p_2) e^{ik_z z_a} + H(z'_b - (z'_2 + \varepsilon_1)) R'_{12}(p_2) e^{ik_z z'_b} \right] \delta(k_2 - k_s).
\end{aligned} \tag{36}$$

The second integral in the algorithm is

$$\begin{aligned}
& \int_{-\infty}^{z'_1 - \varepsilon_2} dz'_2 e^{ik_z z'_2} [R_{01}(p_3)\delta(z'_2 - z_a) + R'_{12}(p_3)\delta(z'_2 - z'_b)] \delta(k_1 - k_2) \\
&\times \left[ H(z_a - (z'_2 + \varepsilon_1)) R_{01}(p_2) e^{ik_z z_a} + H(z'_b - (z'_2 + \varepsilon_1)) R'_{12}(p_2) e^{ik_z z'_b} \right] \delta(k_2 - k_s) \\
&= R_{01}(p_2) R_{01}(p_3) H(z_a - (z'_1 + \varepsilon_2)) \underline{H(z_a - (z_a + \varepsilon_1))} e^{ik_z z_a} e^{-ik_z z_a} \delta(k_1 - k_2) \delta(k_2 - k_s) \\
&+ R_{01}(p_2) R'_{12}(p_3) H((z'_1 - \varepsilon_2) - z_a) H(z'_b - (z_a + \varepsilon_1)) e^{ik_z z'_b} e^{-ik_z z_a} \delta(k_1 - k_2) \delta(k_2 - k_s) \\
&+ R'_{12}(p_2) R_{01}(p_3) H((z'_1 - \varepsilon_2) - z'_b) \underline{H(z_a - (z'_b + \varepsilon_1))} e^{ik_z z_a} e^{-ik_z z'_b} \delta(k_1 - k_2) \delta(k_2 - k_s) \\
&+ R'_{12}(p_2) R'_{12}(p_3) H((z'_1 - \varepsilon_2) - z'_b) \underline{H(z'_b - (z'_b + \varepsilon_1))} e^{ik_z z'_b} e^{-ik_z z'_b} \delta(k_1 - k_2) \delta(k_2 - k_s)
\end{aligned} \tag{37}$$

where all the underlined terms are zero.

The last integral over depth  $z$  in the calculation of  $b_3$  is

$$\begin{aligned}
& \int_{-\infty}^{\infty} e^{ik_z z'_1} [R_{01}(p_1)\delta(z'_1 - z_a) + R'_{12}(p_1)\delta(z'_1 - z'_b)] \delta(k_g - k_1) \\
&\times R_{01}(p_2) R'_{12}(p_3) H((z'_1 - \varepsilon_2) - z_a) H(z'_b - (z_a + \varepsilon_1)) e^{ik_z z'_b} e^{-ik_z z_a} \delta(k_1 - k_2) \delta(k_2 - k_s) \\
&= R_{01}(p_1) R_{01}(p_2) R'_{12}(p_3) \underline{H(-\varepsilon_2)} H(z'_b - (z_a + \varepsilon_1)) e^{ik_z z_a} \delta(k_g - k_1) \delta(k_1 - k_2) \delta(k_2 - k_s) \\
&+ R'_{12}(p_1) R_{01}(p_2) R'_{12}(p_3) e^{ik_z (2z'_b - z_a)} H(z'_b - (z_a + \varepsilon_2)) H(z'_b - (z_a + \varepsilon_1)) \delta(k_g - k_1) \delta(k_1 - k_2) \delta(k_2 - k_s) \\
&= R'_{12}(p_1) R_{01}(p_2) R'_{12}(p_3) e^{2ik_z z'_b} e^{-ik_z z_a} \delta(k_g - k_1) \delta(k_1 - k_2) \delta(k_2 - k_s)
\end{aligned} \tag{38}$$

where we have used the fact that the underlined term is zero and that the last two Heaviside functions are identically equal to 1.

The result for the  $b_3$ , and hence the predicted first order internal multiple, is

$$b_3(p, \omega) = e^{2ik_z z'_b} e^{-ik_z z_a} \int_{-\infty}^{\infty} dk_1 \int_{-\infty}^{\infty} dk_2 R'_{12}(p_1) R_{01}(p_2) R'_{12}(p_3) \delta(k_g - k_1) \delta(k_1 - k_2) \delta(k_2 - k_s), \tag{39}$$

or, after evaluating the integrals and using the relationship between  $p_1$ ,  $p_2$ ,  $p_3$  and  $p$ ,

$$b_3(p, \omega) = R_{12}^{\prime 2}(p) R_{01}(p) \delta(k_g - k_s) e^{2ik_z z'_b} e^{-ik_z z_a}. \tag{40}$$

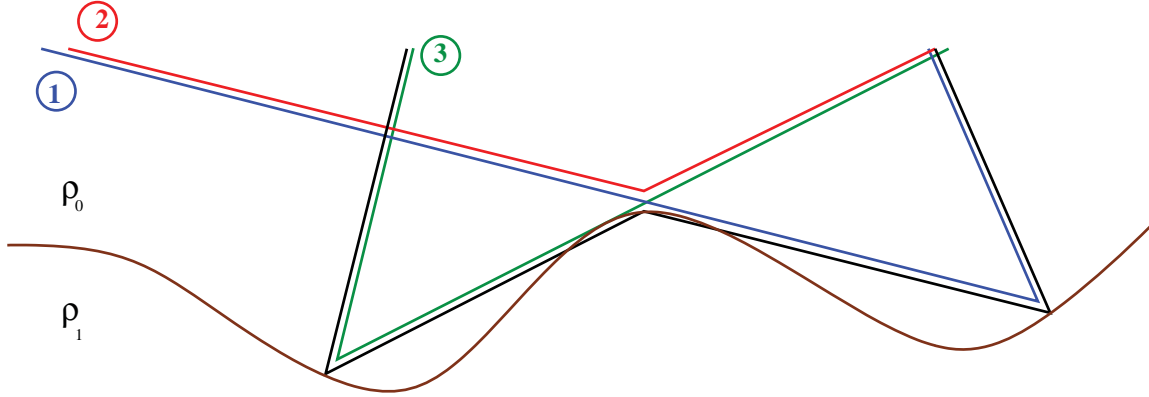


Figure 9: A 2D earth model with an internal multiple satisfying the time monotonicity in the vertical time but not in the total travel time

Recalling that  $R_{12}^2(p) = T_{01}(p)R_2(p)T_{10}(p)$  we find the final result to be

$$b_3(p, \omega) = T_{01}^2(p)R_2^2(p)T_{10}^2(p)R_{01}(p)\delta(k_g - k_s)e^{2ik_z z'_b}e^{-ik_z z_a} \quad (41)$$

consistent with the 1D normal incident result of (20). Integrating over  $k_h$  gives the prediction of the first order internal multiple in space frequency domain

$$IM_{predicted}^{1st}(x_h, 0; \omega) = \frac{1}{2\pi} \int_{-\infty}^{\infty} dk_h \frac{T_{01}^2 R_{12}^2 T_{10}^2 R_{10} e^{2i\nu_1(z_b - z_a)}}{iq_s} e^{ik_h x_h} e^{ik_z z_a}. \quad (42)$$

Comparing this expression with Equation (15) for the actual multiple we see that the predicted multiple has the correct total time and a well approximated amplitude. The amplitude of the predicted multiple in the  $p$ -domain is within a  $T_{01}(p)T_{10}(p)$  factor, a factor which is always close to, but always less than, 1. An integration over the horizontal wavenumber  $k_h$  will average these amplitudes and will result in the predicted amplitude in the space domain which again is going to be lower than, but close to, the actual amplitude of the internal multiple. In addition, since the phase and amplitude construction is performed in the plane waves domain, the internal multiples with headwaves sub-events are also predicted by the algorithm.

In the next section we will further discuss the lower-higher-lower relationship between the pseudo-depths of the sub-events and the similarities and differences of this relationship in total travel time and vertical or intercept time.

## Vertical time and total travel time monotonicity: a 2D example

Consider the earth model shown in Figure 9. For simplicity we assume that only the density  $\rho$  varies at the interface and it has the value  $\rho_0$  in the reference medium and  $\rho_1$  in the actual medium. The velocity is constant  $c_0$ . The actual internal multiple is shown in black and the sub-events composing the multiple are shown in green, blue and red. First, notice that the total traveltime of the shallower reflection (the red event) is bigger than both deeper reflection (green and blue) due to the large

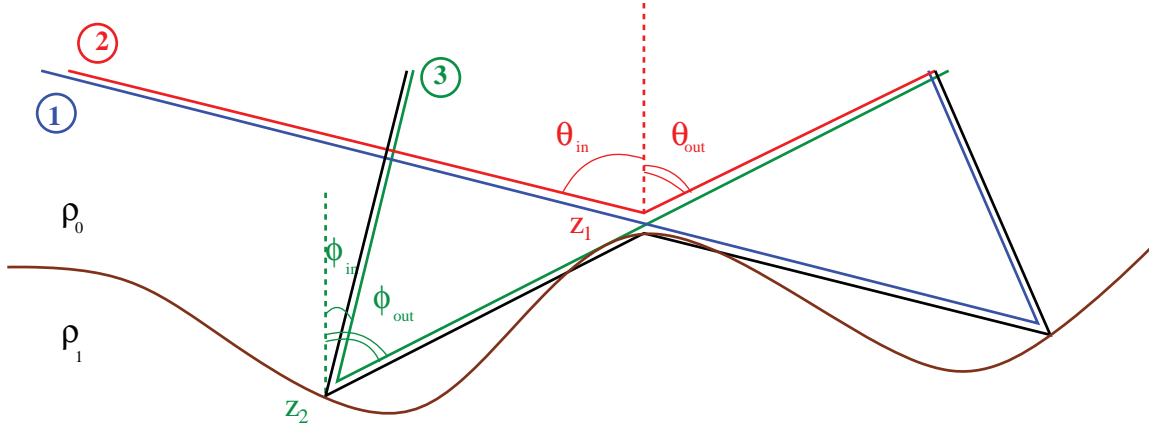


Figure 10: A 2D earth model with an internal multiple satisfying the time monotonicity in the vertical time but not in the total travel time

offsets needed to record such an event. This implies that the longer-shorter-longer relationship is not satisfied by these particular sub-events in the total traveltime.

Next we calculate the vertical times for individual sub-events. The vertical time for the red event along the left leg is (see Figure 10)

$$\tau_{red}^1 = z_1 \frac{\cos \theta_{in}}{c_0} \quad (43)$$

and along the right leg is

$$\tau_{red}^2 = z_1 \frac{\cos \theta_{out}}{c_0}. \quad (44)$$

Summing the two legs we find the total vertical time along the red event to be

$$\tau_{red} = \frac{z_1}{c_0} (\cos \theta_{in} + \cos \theta_{out}). \quad (45)$$

Similarly, for the green event we have

$$\tau_{green} = \frac{z_2}{c_0} (\cos \phi_{in} + \cos \phi_{out}). \quad (46)$$

Since the velocity is constant,  $\theta_{out} = \phi_{out}$ ; we also have that  $\phi_{in} < \theta_{in}$ , and hence  $\cos \phi_{in} > \cos \theta_{in}$ , and  $z_2 > z_1$  which results in

$$\tau_{green} > \tau_{red}. \quad (47)$$

It is not difficult to see that similarly, for this example, we have

$$\tau_{blue} > \tau_{red} \quad (48)$$

where  $\tau_{blue}$  is the vertical time of the blue primary in Figure 10.

The conclusion is that for this model and particular internal multiple, the longer-shorter-longer relationship is satisfied by the vertical or intercept times of the three subevents but not by their total traveltimes. According to equation (10), this relation translates into the lower-higher-lower relationship between the pseudo-depths of the sub-events and hence the internal multiple depicted

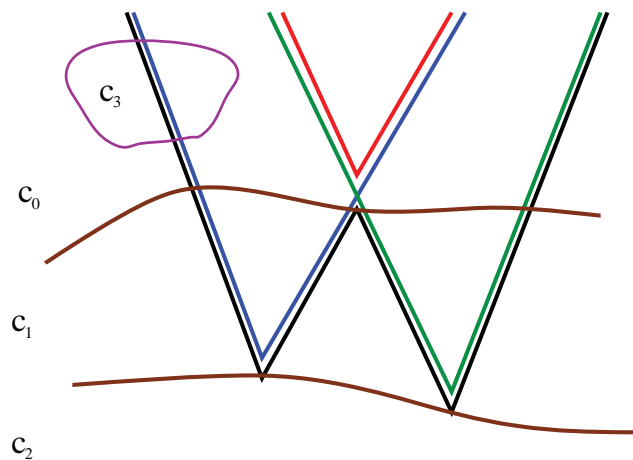


Figure 11: A 2D earth model with an internal multiple containing sub-events which do not satisfy the time monotonicity in either total traveltime or vertical time.

in Figure 9 will be predicted by the inverse scattering internal multiple attenuation algorithm in Equation (3).

In the next section we discuss an earth model and a particular internal multiple in which the longer-shorter-longer relationship in vertical and total travel time is not satisfied.

## Breaking the time monotonicity: a 2D example

Consider the earth model shown in Figure 11 where  $c_0 < c_1$ . A high velocity zone, in which the propagation speed  $c_3$  is much higher than  $c_0$ , intersects one leg of the internal multiple and hence one leg of one of the sub-events (the blue primary in Figure 11). Due to this high velocity zone and the fact that  $c_0 < c_1$ , one can easily imagine a situation in which both the total and the vertical time of the blue primary are shorter than the total and vertical times respectively of the red primary. In this case the lower-higher-lower relationship between the pseudo-depths of the sub-events is not satisfied and hence the internal multiple shown in the picture will not be predicted. The monotonicity is in consequence broken, since even though the actual depths still satisfy a lower-higher-lower relationship, the pseudo-depths, vertical times or total times of the sub-events do not.

To better understand the multiples which do not satisfy the pseudo-depth/vertical-time monotonicity condition and to expand the algorithm to address them, one has to study their creation in the forward scattering series. As indicated by Matson (10) (11) and Weglein et al. (20) the lower-higher-lower relationship in pseudo-depth  $z$  was pointed to by the forward scattering series: the first order approximation to an internal multiple is constructed in the forward scattering series from interactions with point scatterers which satisfy the lower-higher-lower relationship in actual depth. It would be interesting to analyze how a multiple that breaks the monotonicity assumption is constructed by the forward series and to determine if an analogy between the forward and the inverse process would be useful to expand the algorithm to address these kind of events. This particular issue and others will be the subject of future research.

## Conclusions

In this paper we presented an analytic analysis of the inverse scattering internal multiple attenuation algorithm for multi dimensional media. We particularly focused on the mechanism of predicting amplitude and phase properties of an interbed multiple. We have presented the first prestack analysis with analytical data which shows the ability of the algorithm to exactly predict the time and well approximate the amplitude of internal multiples, including the ones with headwaves sub-events. We have discussed in detail the pseudo-depth/vertical-time monotonicity condition and compared it with a similar total traveltime relation. Furthermore, we showed that this restriction on the sub-events can be too strong and could prevent the prediction of some complex internal multiples.

This research is an important step forward in better understanding the inverse scattering series and the internal multiple attenuation algorithm derived from it. The analytic analysis presented, targets internal multiples which occur in complex multi-dimensional media. Having a better understanding of the structure and definition of such internal multiples opens up new possibilities of identifying, predicting and subtracting them from the collected data. The inverse scattering series is presently the only tool that can achieve these objectives without any knowledge about the actual medium.

## Acknowledgments

This work was partially supported by NSF-CMG award number DMS-0327778. The support of M-OSRP sponsors is also gratefully acknowledged. Adriana C. Ramírez is thanked for providing the earth model in Figure 9. Jon Sheiman, Einar Otnes and Fons ten Kroode are acknowledged for their useful comments and insights on this work.

## References

- [1] K. AKI, P. G. RICHARDS (1980), *Quantitative Seismology*, W. H. Freeman and Company, San Francisco.
- [2] F. V. ARAUJO (1956), *Linear and Nonlinear Methods Derived from Scattering Theory: Backscattered Tomography and Internal Multiple Attenuation*, Ph.D. thesis, Department of Geophysics, Universidad Federal de Bahia, Salvador-Bahia, Brazil, 1994 (in Portuguese).
- [3] R. N. BRACEWELL (1956), *Strip integration in radio astronomy*, Aust. J. Phys., Vol. 9, pp. 198-217.
- [4] R. N. BRACEWELL, A. C. RIDDLE (1967), *Inversion of fan-beam scans in radio astronomy*, Astrophys. J., Vol. 150, pp. 427-434.
- [5] C. G. M. BRUIN, C. P. A. WAPENAAR, A. J. BERKHOUT (1990), *Angle-dependent reflectivity by means of prestack migration*, Geophysics, Vol. 55, No. 9, pp. 1223-1234.

- [6] P. M. CARVALHO (1992), *Free Surface Multiple Reflection Elimination Method Based on Nonlinear Inversion of Seismic Data*, Ph.D. thesis, Department of Geophysics, Universidad Federal de Bahia, Salvador-Bahia, Brazil, (in Portuguese).
- [7] J. B. DIEBOLD AND P. L. STOFFA (1981), *The travelttime equation, tau-p mapping, and inversion of common midpoint data*, Geophysics, Vol. 46, No. 3, pp. 238-254.
- [8] S. T. KAPLAN, K. A. INNANEN, E. OTNES AND A. B. WEGLEIN (2005), *Internal multiple attenuation code-development and implementation project report*, M-OSRP Annual Report, 2005.
- [9] A. MALCOLM AND M. V. DE HOOP (2005), *A method for inverse scattering based on the generalized Bremmer coupling series*, Inverse Problems, submitted
- [10] K. H. MATSON (1996), *The relationship between scattering theory and the primaries and multiples of reflection seismic data*, J. Seismic Exploration, 5, pp. 63-78.
- [11] K. H. MATSON, *An Inverse Scattering Series Method for Attenuating Elastic Multiples from Multicomponent Land and Ocean Bottom Seismic Data*, Ph.D. thesis, Department of Earth and Ocean Sciences, University of British Columbia, Vancouver, BC, Canada, 1997.
- [12] B. G. NITA AND A. B. WEGLEIN (2004), *Imaging with  $\tau = 0$  versus  $t = 0$ : implications for the inverse scattering internal multiple attenuation algorithm*, SEG Expanded Abstracts, 74<sup>th</sup> Annual Meeting of the Society for Exploration Geophysicists, Denver, Colorado.
- [13] A. C. RAMÍREZ AND A. B. WEGLEIN (2005), *Progressing the analysis of the phase and amplitude prediction properties of the inverse scattering internal multiple attenuation algorithm*, submitted to Journal of Seismic Exploration.
- [14] A. C. RAMÍREZ AND A. B. WEGLEIN (2005),
- [15] R. STOLT (1978), *Migration by Fourier transform*, Geophysics, 43, pp. 23-48.
- [16] R. STOLT AND A. B. WEGLEIN (1985), *Migration and inversion of seismic data*, Geophysics, 50, pp. 2458-2472.
- [17] A. P. E. TEN KROODE (2002), *Prediction of internal multiples*, Wave Motion, 35, pp. 315-338.
- [18] S. TREITEL, P. R. GUTOWSKI AND D. E. WAGNER (1982), *Plane-wave decomposition of seismograms*, Geophysics, Vol. 47, No. 10, pp. 1374-1401.
- [19] A. B. WEGLEIN, F. A. GASPAROTTO, P. M. CARVALHO, R. H. STOLT (1997), *An inverse scattering series method for attenuating multiples in seismic reflection data*, Geophysics, 62, pp. 1975-1989.
- [20] A. B. WEGLEIN, F. V. ARAUJO, P. M. CARVALHO, R. H. STOLT, K. H. MATSON, R. COATES, D. CORRIGAN, D. J. FOSTER, S. A. SHAW, H. ZHANG (2003), *Inverse scattering series and seismic exploration*, Topical Review Inverse Problems, 19, pp. R27-R83.
- [21] A. B. WEGLEIN, W. DRAGOSSET (2005), *Internal Multiples*, SEG Reprint Volume.